processes

MDPI

*Article*

# Improved Laccase Encapsulation in Copper-Doped Zeolitic Imidazolate Framework-8 for Reactive Black 5 Decolorization

**Shuyu Yu [1], Yibo Lu [2], Dandan Du [1], Rankun Wu [3], Xiang Ji [1,4] and Hao Li [1,*]**

[1] College of Water Conservancy and Civil Engineering, Inner Mongolia Agricultural University, Hohhot 010018, China; yushuyu@imau.edu.cn (S.Y.); duddpublic@163.com (D.D.); jixiang@imau.edu.cn (X.J.)
[2] College of Life Sciences, Northeast Forestry University, Harbin 150040, China; woshiyu2001@163.com
[3] Comprehensive Support and Technology Extension Center, Xi-Doupu Town, Baotou 014214, China; nmg_wuchun@163.com
[4] Hetao College, Bayannur 015000, China
* Correspondence: hao.li@imau.edu.cn

**Abstract:** As the largest group of synthetic dyes, azo dyes can pose various health and environmental risks due to their widespread use and challenging degradation. Laccases are efficient green biocatalysts for the degradation of organic pollutants. Herein, we report the *in situ* packaging of laccase in copper-doped zeolitic imidazolate framework-8 (ZIF-8) for the decolorization of reactive black 5, which is a model azo dye. The immobilization support (Cu5/mZIF-8) was obtained via lowering the precursor ratio of ZIF-8 and incorporating copper ions during the synthesis process. Cu5/mZIF-8 were found to be nanospheres with an average diameter of around 150 nm. Laccase encapsulated in Cu5/mZIF-8 showed an activity recovery of 75.6%, which was 2.2 times higher than that of the laccase embedded in ZIF-8. Meanwhile, the immobilized laccase (Lac@Cu5/mZIF-8) showed a higher catalytic activity in organic solvents than that of the free enzyme. In the presence of a mediator, Lac@Cu5/mZIF-8 could remove 95.7% of reactive black 5 in 40 min. After four consecutive cycles, the dye decolorization efficiency declined to 28%. About four transformation products of reactive black 5 were identified via LC-MS analysis, and the potential decolorization mechanism was proposed. The results indicated that the immobilized laccase could be used as an efficient biocatalyst in dye decolorization.

**Keywords:** laccase; zeolitic imidazolate framework-8; immobilization; dye decolorization



**Citation:** Yu, S.; Lu, Y.; Du, D.; Wu, R.; Ji, X.; Li, H. Improved Laccase Encapsulation in Copper-Doped Zeolitic Imidazolate Framework-8 for Reactive Black 5 Decolorization. *Processes* **2023**, *11*, 2937. https://doi.org/10.3390/pr11102937

Academic Editor: Juan Carlos Moreno-Piraján

Received: 5 September 2023
Revised: 25 September 2023
Accepted: 4 October 2023
Published: 10 October 2023



## 1. Introduction

Synthetic dyes are widely used in a variety of industries, such as textiles, printing, and food processing [1,2]. The global annual production of dyes is estimated to be $7 \times 10^7$ tons, and most of the dyes are consumed by the textile industry [2]. About 10–25% of textile dyes are discharged in wastewater during the dyeing process. These dye-containing effluents cause serious environmental hazards due to the recalcitrant and toxic nature of most synthetic dyes [1]. According to their chemical structure, synthetic dyes can be categorized into different groups, such as azo, anthraquinone, and triphenylmethane dyes [1,2]. Azo dyes comprise the largest group among various commercial dyes, accounting for more than 70% of annual dye production [3]. Azo dyes contain one or more azo bonds (-N=N-) that are linked to aromatic compounds. These dyes are generally very stable in the environment and show adverse effects on the ecosystem and human health [3,4]. Trace amounts of azo dyes in water bodies can reduce the penetration of sunlight and impair photosynthetic activity, leading to a decrease in dissolved oxygen and growth inhibition in aquatic life [2]. Furthermore, the primary metabolites of azo dye degradation are toxic aromatic amines, which are derived from the breakage of azo bonds and have potential carcinogenic and mutagenic properties [3,4]. Therefore, it is of great concern to remove azo dyes from wastewater to reduce their influence on the environment.

A variety of techniques have been developed for the treatment of wastewater containing azo dyes, including physicochemical, biological, and electrochemical processes [2–4]. Although some of the physical and chemical methods are effective in the treatment of azo dye effluents, these approaches have some drawbacks, such as high costs, the formation of hazardous byproducts, and problematic waste disposal [2,4]. Biological processes offer considerable potential for solving these problems, owing to their ecologically favorable and low-cost nature. The biodegradation of azo dyes mainly relies on the capability for microbial transformation, which disrupts the original dye structure via enzyme-catalyzed reactions [3]. However, this treatment process can sometimes be time-consuming due to the low growth rate and activity of microorganisms, which are often affected by the toxicity of dyes, nutrient sources, or environmental conditions. In comparison, the enzyme-based strategy is more efficient and straightforward in dye degradation and also produces less sludge. As a result, the enzymatic method has been explored as a prospective solution for dye wastewater treatment [5–7].

Several microbial enzymes, such as azoreductases, laccases, and peroxidases, are involved in the transformation of azo dyes [5,7,8]. In recent years, laccases have shown great potential in the decolorization of different textile dyes, including azo dyes. Laccases (EC 1.10.3.2) belong to the broader family of multicopper oxidases [9]. These enzymes have a broad substrate range and they do not need other cofactors for activation compared with azoreductases or peroxidases. Moreover, laccases catalyze azo dyes through a highly nonspecific free radical mechanism, generating phenolic compounds instead of toxic aromatic amines [5,8,10]. Despite these advantages, the application of laccases is often restricted by their low stability and lack of recyclability. Enzyme immobilization is an efficient strategy to overcome these limitations, which enables the provision of stable biocatalysts with an improved reusability [10]. Laccases have been immobilized on a large number of carriers for dye decolorization, including natural polymers, inorganic nanomaterials, and metal–organic frameworks [10,11].

Metal–organic frameworks (MOFs) are excellent supports for enzyme immobilization, owing to their large pore volume and tunable structure [12]. Additionally, MOFs are frequently used as adsorbents for pollutant removal from wastewater [13,14]. Therefore, the integration of MOFs with enzymes might increase the pollutant removal efficiency. Some MOFs can be prepared under biocompatible conditions and enable the assembly of MOFs around enzymes during the synthesis process. The frequently used MOFs for this purpose include zeolitic imidazolate frameworks (ZIFs), HKUST-1, and MIL-53. In particular, ZIF-8 is the most widely used MOF for the *in situ* encapsulation of enzymes [11,12]. However, the small pore-aperture size of ZIF-8 (3.4 Å) often results in severe mass transfer limitations in enzymatic reactions. For instance, laccase embedded in ZIF-8 exhibited a size-selective substrate specificity. The encapsulated laccase showed no activity against 2,2′-azino-bis(3-ethylbenzothiazoline-6-sulphonic acid) (ABTS), which is not able to enter the pores of ZIF-8. While it could convert two small substrates (2,6-dimethoxyphenol and syringaldazine), the highest activity recovery was rather low (about 11%) [15]. To address this issue, structural defects have been introduced to ZIF-8 to generate larger pores for enzyme encapsulation. ZIF-8 with hierarchical pores favors substrate entrance and product transport and, thus, enhances the catalytic activity of the embedded enzymes [16–18]. However, few laccases have been encapsulated in ZIF-8 with defective structures.

Hierarchical structures in ZIF-8 can be generated using template-based or template-free strategies [16,18]. It has been reported that the precursor concentrations and ratios play a vital role in the crystallization of ZIF-8 [19]. As a result, structural defects could be introduced to ZIF-8 through simply controlling the precursor concentrations during the synthetic process [16,17]. Previously, we successfully expressed a laccase gene from *Bacillus amyloliquefaciens* in *Escherichia coli*. The recombinant laccase could be produced with a high yield in the culture supernatant [20]. In this work, we aimed to improve the *in situ* encapsulation of the recombinant laccase in modified ZIF-8 (mZIF-8) and achieve its repeated use in dye decolorization. We synthesized mZIF-8 at low precursor concentrations and further

investigated the effect of copper ions on the preparation of laccase@mZIF-8 composites. The resulting immobilized laccase (Lac@Cu5/mZIF-8) was characterized via Fourier-transform infrared spectroscopy (FT-IR), X-ray diffraction (XRD), and thermogravimetric analysis (TGA). Finally, the prepared biocomposites were utilized for azo dye decolorization, and the transformation products were identified via liquid chromatography–mass spectrometry (LC-MS).

## 2. Materials and Methods

### 2.1. Materials

Syringaldazine, reactive black 5, acetosyringone, and 2-methylimidazole (2-MeIM) were obtained from Sigma-Aldrich (Shanghai, China). Zinc acetate dehydrate, zinc nitrate hexahydrate, and copper acetate monohydrate were products of Aladdin (Shanghai, China). Other chemicals were of analytical reagent grade. The recombinant laccase of *Bacillus amyloliquefaciens* was purified as previously described [20].

### 2.2. Immobilization of Laccase

The conventional laccase-ZIF-8 biocomposites (Lac@ZIF-8) were prepared via a water-based approach [21]. The purified laccase (0.5 mL) and zinc nitrate solution (0.31 M, 0.5 mL) were added into 2-MeIM (1.25 M, 5 mL). The mixture was then stirred at room temperature for 1 h. The product was collected via centrifugation at 12000 rpm for 10 min, and washed three times with deionized water. The synthesis of ZIF-8 was similar without laccase addition.

Modified ZIF-8 (mZIF-8) was synthesized according to Wu et al. [16]. Briefly, 2 mL of zinc acetate solution (20 mM) was added into 2 mL of 2-MeIM (80 mM). Then, they were mixed via stirring for 30 min at room temperature. The prepared mZIF-8 was centrifuged at 12,000 rpm for 10 min, followed by washing with deionized water. Encapsulation of laccase in mZIF-8 (Lac@mZIF-8) was conducted similarly by including 0.6 mL of purified laccase in the reaction system. The effect of copper on laccase immobilization was assessed via the preparation of a zinc acetate solution (20 mM) containing different molar ratios of copper acetate. Then, the metal acetate solutions were mixed with laccase and 2-MeIM to obtain encapsulated laccases. The copper-doped supports prepared with 5:100, 10:100, and 15:100 Cu:Zn ratios will be denoted as Cu5/mZIF-8, Cu10/mZIF-8, and Cu15/mZIF-8, respectively. The immobilized laccase with the highest activity recovery was selected for further study.

### 2.3. Laccase Activity Assay

Laccase activity was measured at 30 °C using syringaldazine as the substrate [22]. The oxidation of syringaldazine (0.1 mM) was measured at 525 nm ($\varepsilon_{525}$ = 65,000 $M^{-1}$ $cm^{-1}$) in 0.1 M citrate–phosphate buffer with a UV-2100 spectrophotometer (Shanghai Spectrum, Shanghai, China). One unit of enzyme activity was defined as the amount of enzyme required to oxidize 1 μmol of substrate per minute.

### 2.4. Characterization of Immobilized Laccase

#### 2.4.1. Scanning Electron Microscopy (SEM)

The morphology of synthesized supports was observed via SEM using a JSM-6700F instrument at an accelerating voltage of 5 kV in high-vacuum mode (JEOL, Tokyo, Japan). The samples were coated with gold via sputtered deposition prior to SEM observation.

#### 2.4.2. XRD Analysis

The XRD results of the samples were obtained via an X'Pert 3 Powder diffractometer (PANalytical, Almelo, The Netherlands) using Cu Kα radiation (λ1 = 1.5406 Å, λ2 = 1.5444 Å, 40 kV, 40 mA) with a step size of 2 °C/min and a 2θ range from 5 to 40°.

#### 2.4.3. FT-IR Spectra

FT-IR spectra were recorded via a Nicolet is50 spectrophotometer (Thermo Fisher Scientific, Waltham, MA, USA) in transmission mode at ambient temperature. The samples were mixed with KBr, were pressed to disc, and underwent FTIR analysis. The measurement parameters were set as follows: spectral range, 4000–400 $cm^{-1}$; resolution, 4 $cm^{-1}$; number of spectrum accumulations, 32.

#### 2.4.4. TGA Analysis

TGA measurements were performed using an STA449 F3 analyzer (Netzsch, Selb, Germany). The samples were heated from room temperature to 800 °C at a rate of 5 °C/min under an atmosphere of air.

#### 2.4.5. Enzyme Characterization

The optimal pH and temperature of the immobilized laccase were measured via the determination of the laccase activities at various pH values and temperatures, as previously described [20]. The kinetic parameters of the immobilized enzyme were assayed at 30 °C, using different concentrations of syringaldazine (5–100 μM). The effects of organic solvents on the laccase activity were determined via the incorporation of 10% (*v*/*v*) of organic solvents into the enzyme assay mixture. The laccase activity in the absence of organic solvents was recorded as 100%. All assays were carried out in triplicate.

### *2.5. Dye Decolorization*

Dye decolorization was conducted using reactive black 5 as the model azo dye. The reaction mixture (2 mL) contained 20 mg/L of dye, 0.1 mol/L Tris-HCl buffer (pH 7.0), and laccase (100 U/L). The mediator effect on dye decolorization was tested via the inclusion of 0.1 mM of acetosyringone in the reaction system. Reactions were initiated via the addition of laccase and incubated at 30 °C under shaking conditions (150 rpm). Control samples were run in parallel without the addition of laccase. The reusability of the immobilized laccase was evaluated in batch mode. After each cycle (40 min), the immobilized laccase was recovered through centrifugation (12,000 rpm, 10 min) without washing. Then, the immobilized laccase was resuspended in a fresh reaction containing Tris-HCl buffer (0.1 mol/L, pH 7.0), reactive black 5 (20 mg/L), and acetosyringone (0.1 mM) to start a new decolorization cycle. Dye decolorization was determined at 597 nm with a UV-2100 spectrophotometer. All reactions were performed in triplicate. The decolorization percentage was defined as follows:

$$\text{Decolorization percentage (\%)} = (A_0 - A)/A_0 \times 100$$

where $A_0$ is the dye absorbance of the control, and A is the dye absorbance of the reaction sample.

### *2.6. Identification of Decolorization Products*

The decolorization products were collected via centrifugation at 12,000 rpm for 10 min. The supernatants were filtered through a 0.45 μm membrane filter and used for further analysis. The identification of transformation products was achieved using a Vanquish high-performance liquid chromatography (HPLC) system coupled to a Q Exactive Focus mass spectrometry system (Thermo Fisher Scientific, Waltham, MA, USA). The HPLC separation was performed using a Hypersil GOLD column (100 × 2.1 mm, 1.9 μm, Thermo Fisher Scientific, Waltham, MA, USA), with an injection volume of 5 μL and a flow rate of 0.35 mL/min. The mobile phases were 0.1% formic acid (A) and methanol (B), using the following gradient elution (A/B, *v*/*v*): 98:2 at 0–1 min, 2:98 at 9–12 min, and 98:2 at 13–15 min. The MS analysis was performed with an electrospray ionization source with a spray voltage of 3.0 kV, and a capillary temperature of 320 °C. The MS acquisition was processed in full scan mode from 70 to 1000 Da, with a mass resolution of 70,000. The mass spectra were processed using the Xcalibur 4.1 software (Thermo Fisher Scientific).

## 3. Results and Discussion

### *3.1. Preparation of Immobilized Laccase*

ZIF-8 can be synthesized in water via simply mixing zinc ions with 2-MeIM at room temperature. This property greatly favors their application in the one-pot immobilization of enzymes [11,12]. Laccases from different sources have been encapsulated in ZIF-8 [11]. However, laccase encapsulated in ZIF-8 may suffer from a strong diffusion barrier and exhibits a low catalytic activity because of the small pore window size of ZIF-8 [15]. The structural evolution of the protein-ZIF-8 composite involves two key amorphous phases, including 2-MeIM/Zn amorphous particles and protein/2-MeIm/Zn particles [19]. Amorphous particles form at low 2-MeIM/Zn ratios or low precursor concentrations instead of highly crystalline ZIF-8 [16,19]. In this case, the protein-triggered crystallization of ZIF-8 exhibits a multiphase structure containing amorphous phase and coordination-defected units, which favors substrate entrance [16,23]. Therefore, we prepared modified ZIF-8 (mZIF-8) for laccase encapsulation by introducing structural defects into ZIF-8, which was achieved through decreasing the concentrations of 2-MeIM [16]. Compared with the conventional ZIF-8 support, mZIF-8 showed an improved activity recovery for laccase immobilization. The laccase encapsulated in the ZIF-8 and mZIF-8 showed an activity recovery of 34.9% and 63.9%, respectively (Figure 1). Using the same approach, Wu et al. found that glucose oxidase, catalase, and lipase encapsulated in the amorphous ZIF-8 exhibited almost 100% relative activity compared to the free enzymes, which was about 5–20 times higher than that of those immobilized in ZIF-8 [16]. The results proved that structural defects introduced into ZIF-8 could greatly enhance substrate accessibility for the embedded enzymes.

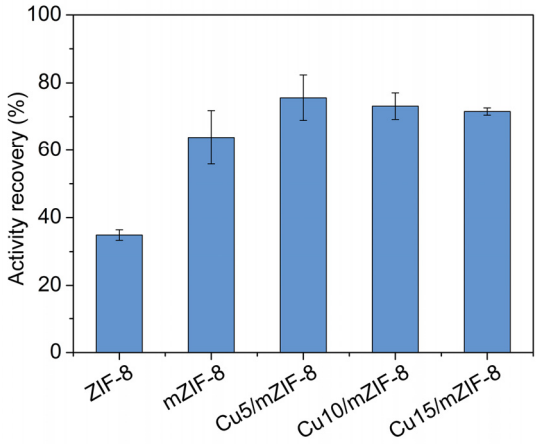


**Figure 1.** The activity recovery of laccases encapsulated in the different supports.

As laccases are copper-containing enzymes, copper ions play a vital role in substrate oxidation for laccases [24]. Some laccases immobilized in Cu-MOFs demonstrated high activity owing to the synergistic effect between the laccases and copper nanoparticles [11]. For example, the laccase embedded in Cu-BTC showed a 16.5-fold activity in comparison with the same amount of free laccase [25]. We tested the effect of introducing copper into mZIF-8 on the laccase activity. Copper-doped ZIF-8 can be easily achieved through the incorporation of copper ions into the synthesis process of ZIF-8, which leads to the simultaneous partial substitution of zinc by copper ions [26,27]. The activity recoveries of laccase embedded in copper-doped mZIF-8 supports are presented in Figure 1. The incorporation of copper into mZIF-8 further increased the activity of immobilized laccase. A Cu:Zn ratio of 5:100 led to the highest activity recovery (75.6%) for laccases encapsulated in copper-doped mZIF-8, which was about 2.2 times higher than that of those immobilized in ZIF-8. Further increases in the copper content showed no improvement in the laccase activity (Figure 1). The resulting copper-doped biocomposites (Lac@Cu5/mZIF-8) were used for enzyme characterization and dye decolorization.

### *3.2. Characterization of Immobilized Laccase*

The precursor concentrations affect both the size and morphology of ZIF-8 materials [19,28]. The ZIF-8 particles synthesized at high precursor concentrations appeared as rhombic dodecahedrons, with an average size of about 1.5 μm (Figure 2a). After lowering the precursor concentrations, as well as including copper ions, the obtained copper-doped mZIF-8 (Cu5/mZIF-8) exhibited the form of nanospheres, which had an average diameter of around 150 nm (Figure 2b). The size and morphology of Cu5/mZIF-8 were very similar to those of aZIF, which was synthesized at the same precursor concentrations [16].

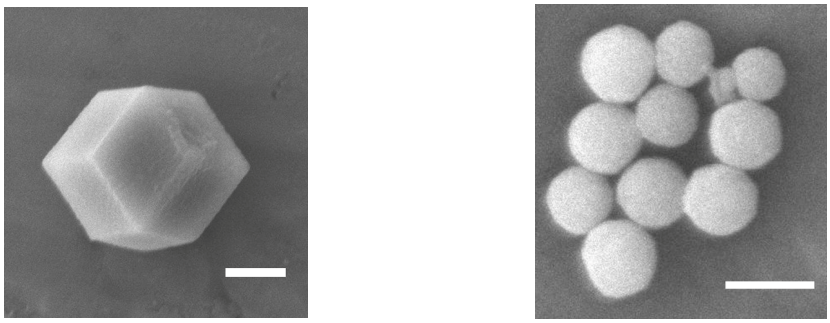

(**a**) (**b**)

**Figure 2.** SEM images of the laccase immobilization support. (**a**) ZIF-8, scale bar 500 nm; (**b**) Cu5/mZIF-8, scale bar 200 nm.

It has been reported that amorphous structures exist in aZIF, so we examined the crystallinity of Cu5/mZIF-8 via XRD analysis. As shown in Figure 3a, ZIF-8 particles exhibited characteristic peaks at 7.2°, 10.2°, 12.5°, 14.6°, 16.3°, 17.8°, 24.3°, and 26.5°, which could be assigned to planes of (011), (002), (112), (022), (013), (222), (233), and (134), respectively. The results confirmed the sodalite structure of ZIF-8 with a high crystallinity [28,29]. Unlike the amorphous structure of aZIF, Cu5/mZIF-8 showed some typical peaks (2θ = 14.7°, 16.4°, 17.9° and 26.5°) of ZIF-8 with a sodalite topology [29,30]. However, the prominent peaks of ZIF-8 at 7.3° and 10.3° were not observed in Cu5/mZIF-8, indicating that the growth of (011) and (002) planes was hindered (Figure 3a). According to previous reports, a low 2-MeIM/Zn ratio limited the growth of ZIF-8 (sod) crystals and led to the formation of a ZIF-8 (dia) topology or amorphous ZIF [16,19]. Also, some diffraction peaks of zinc–hydroxide-containing byproducts and other unknown phases could be observed in the XRD patterns of ZIF-8 synthesized at low 2-MeIM/Zn ratios [28,30,31]. After laccase encapsulation, the obtained Lac@Cu5/mZIF-8 exhibited the XRD patterns of both ZIF-8 and Cu/mZIF-8, implying that laccase addition during Cu5/mZIF-8 synthesis favored the formation of ZIF-8 (Figure 3a). The result was in agreement with previous studies on the synthesis of protein-ZIF-8 composites at a low precursor ratio [19,23]. While the 2-MeIM/Zn precursor was unable to crystallize at a low precursor ratio, the proteins directly triggered the nucleation of ZIF-8 crystals [23].

The FT-IR spectra of the supports and immobilized laccase are shown in Figure 3b. The characteristic peak at 423 $cm^{-1}$ corresponding to the Zn-N stretching mode was observed in ZIF-8, Cu5/mZIF-8, and Lac@Cu5/mZIF-8 [30]. The peaks of 995 $cm^{-1}$ and 1581 $cm^{-1}$ are derived from the C-N bending vibration and C=N stretching mode of 2-MeIM, respectively. The stretching mode of the imidazole ring demonstrates a band at 1420 $cm^{-1}$ [30]. Additionally, the FT-IR spectra of these materials show the bands at 650–800 $cm^{-1}$ and 930–1350 $cm^{-1}$, which are associated with the out-of-plane and in-plane bending of the imidazole ring, respectively [30]. The aromatic C-H stretching in the imidazole ring at 3134 $cm^{-1}$ and the aliphatic C-H stretching in the methyl group at 2930 $cm^{-1}$ are also found in the spectra of the tested samples [32]. Compared with ZIF-8, the new peaks of Cu5/mZIF-8 at 499 $cm^{-1}$ and 538 $cm^{-1}$ might be associated with Cu-N bond stretching and vibration, implying the coordination of copper with nitrogen atoms on 2-MeIM [27,33]. For Lac@Cu5/mZIF-8, the

characteristic band at 1655 $cm^{-1}$ resulted from the C=O stretching of amide I, while the peak at 1250 $cm^{-1}$ is ascribed to amide III [30,34]. The results confirmed the successful encapsulation of laccase in Cu5/mZIF-8.

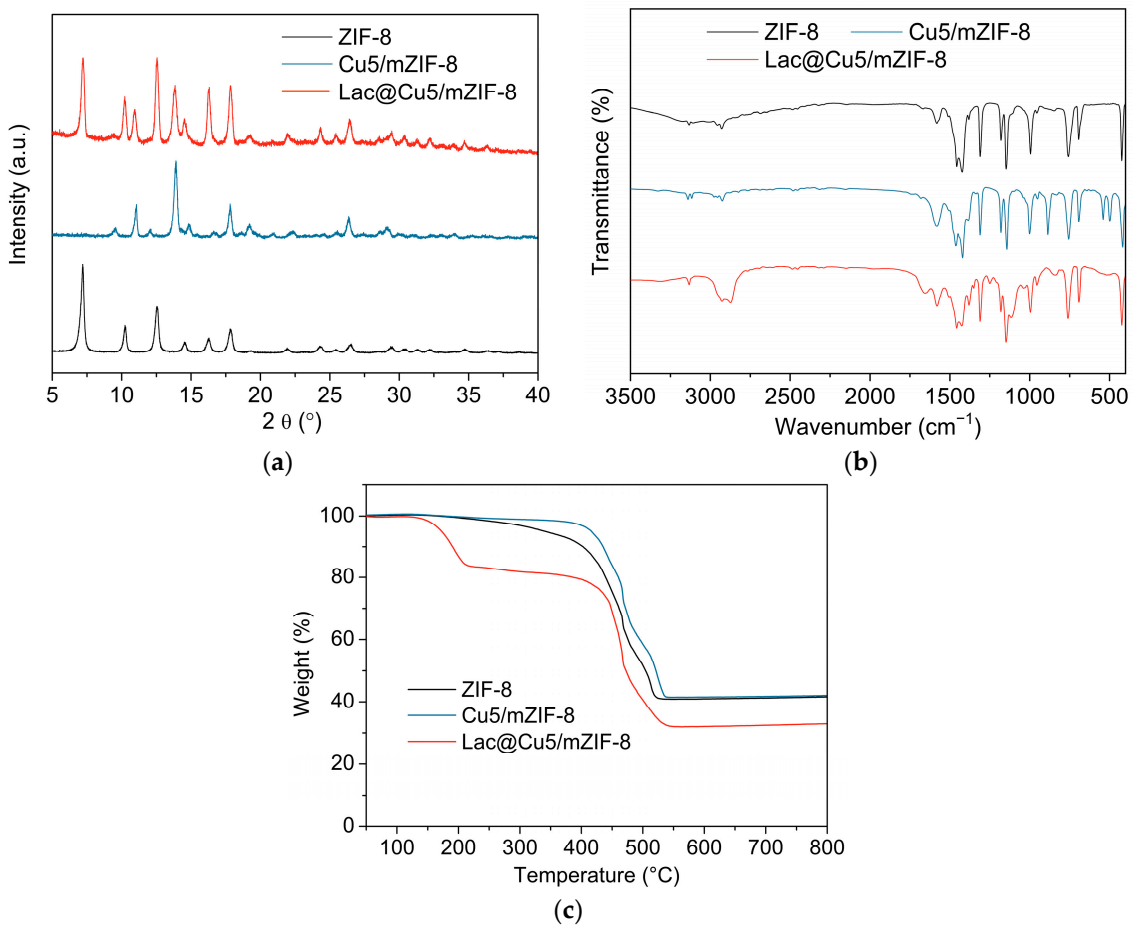


**Figure 3.** The characterization of ZIF-8, Cu5/mZIF-8, and Lac@Cu5/mZIF-8. (**a**) XRD patterns; (**b**) FT-IR spectra; (**c**) TGA curves.

The TGA curve of Cu5/mZIF-8 was very similar to that of ZIF-8 (Figure 3c). While ZIF-8 was rather stable below 400 °C, Cu5/mZIF-8 showed gradual weight loss in the range of 220–400 °C. The result suggested that the thermal stability of Cu5/mZIF-8 was slightly lower than that of ZIF-8, which could be due to the structural defects introduced in Cu5/mZIF-8. Both matrices demonstrated a sharp weight loss between 400 and 530 °C, indicating the structural decomposition of the tested samples [34]. The incorporation of laccase was also supported by the TGA analysis. There are two steps of weight loss of Lac@Cu5/mZIF-8 (Figure 3c). The first step was observed in the temperature range of 130–220 °C, which was attributed to the removal of adsorbed water and unreacted reagents [30,34]. The second weight-loss stage (from about 220 to 400 °C) corresponded to the decomposition of protein molecules [30,35].

### *3.3. Catalytic Performance of Immobilized Laccase*

The catalytic activity of immobilized laccase was compared with that of the free enzyme under different pHs and temperatures. Both the free and immobilized laccase showed an optimum pH of around 6.6. However, the immobilized laccase had a slightly higher activity under more acidic conditions than the free enzyme (Figure 4a). This might be related to the instability of the ZIF support, which tends to decompose below pH 6.0 [36]. As a result, the immobilization matrix displayed a suitable buffering function and alleviated the inactivation of laccase caused by acidic conditions. The immobilized laccase exhibited

the same maximum temperature as its free counterpart, and their temperature profiles for catalytic activity were very similar (Figure 4b). This recombinant laccase has been proved to be a rather thermal stable enzyme, showing a half-life of about 8 h at 60 °C [37]. The good thermostability would facilitate its application in wastewater treatment.

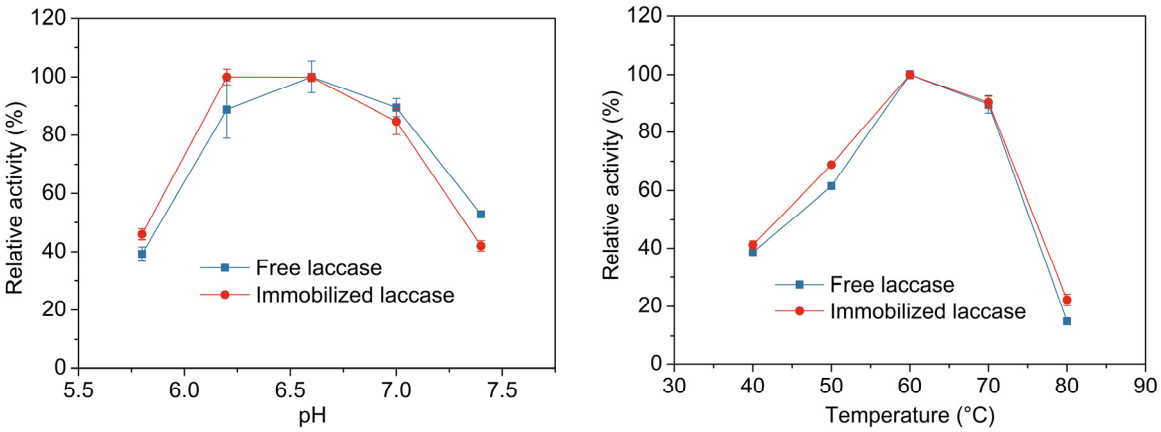


(**a**) (**b**)

**Figure 4.** The effect of the pH and the temperature on the activity of the free and immobilized laccase. (**a**) pH; (**b**) temperature.

The kinetic constants of laccase were estimated from the Lineweaver–Burk plot. The $K_m$ values of the free laccase and immobilized laccase were determined as 18.3 ± 2.8 μM and 21.9 ± 3.5 μM, respectively. The increase in the $K_m$ value suggested that the affinity of the laccase to the substrate decreased after immobilization, which was in agreement with previous studies [38,39]. The reason for the change in substrate affinity might be due to the decline in substrate accessibility to the embedded enzyme [38,39]. Accordingly, a slight decrease in $V_{max}$ was also observed after laccase immobilization. The $V_{max}$ value of the immobilized laccase was 11.6 ± 0.9 nmol/min, while that of the free laccase was 12.2 ± 0.6 nmol/min. The stability of Lac@Cu5/mZIF-8 in common organic solvents was tested using methanol, ethanol, acetone, and acetonitrile. All the tested organic solvents caused an obvious decline in laccase activity; however, Lac@Cu5/mZIF-8 demonstrated higher activity in these organic solvents than that of the free laccase (Table 1).

**Table 1.** The effect of organic solvents on the activity of the free and immobilized laccase.

| Organic Solvent (10%, *v*/*v*) | Residual Activity (%) | |
|---|---|---|
| | Free Laccase | Immobilized Laccase |
| Methanol | 54.6 ± 3.5 | 58.8 ± 1.8 |
| Ethanol | 42.4 ± 1.6 | 44.3 ± 2.6 |
| Acetone | 42.6 ± 2.1 | 45.7 ± 3.0 |
| Acetonitrile | 48.7 ± 2.6 | 51.7 ± 1.7 |

### *3.4. Dye Decolorization*

Reactive black 5 is a toxic and recalcitrant azo dye [40], so we selected it as a model dye to test the decolorization ability of the immobilized laccase. As shown in Figure 5a, reactive black 5 was poorly decolorized by the free and immobilized laccase. Only 9.5% and 14.3% dye removal were achieved after 10 h for the laccase and Lac@Cu5/mZIF-8, respectively. Meanwhile, the result also indicated that reactive black 5 had little adsorption on the immobilization matrix. To facilitate dye decolorization, we included acetosyringone as a laccase mediator in the degradation system. In the presence of the mediator, reactive black 5 could almost be completely decolorized by Lac@Cu5/mZIF-8. About 95.7% decolorization

was reached within 40 min (Figure 5b). Meanwhile, the free laccase could also decolorize about 94% of the tested dye with the help of the mediator. Similar results have been found for other laccases, which required the participation of a mediator for the efficient decolorization of reactive black 5 [41–43]. The reusability of immobilized enzymes can favor their application through reducing operational costs. The recyclability of Lac@Cu5/mZIF-8 was assessed through the performance of several consecutive cycles for reactive black 5 decolorization. The dye decolorization percentage decreased from the third reaction cycle, and only 28% of the dye was removed by the immobilized laccase after four cycles (Figure 5b). The decline in decolorization efficiency was ascribed to the gradual sample loss during the recovery process [38,44]. The immobilized laccase could not be easily recovered via centrifugation because of its small size. A similar result has been observed for glucose oxidase immobilized in ZIF-8 [44]. The immobilized enzyme (GOx/ZIF-8) lost more than 70% of its original activity after just two cycles owing to its nanometer size (around 400 nm). After the introduction of PDA to the synthesis process, the particle size of the immobilized enzyme (PDA@GOx/ZIF-8) increased to 5–40 μm, which greatly facilitated its recovery as well as its reusability [44]. Moreover, the decrease in activity after repeated use might result from enzyme inactivation or product inhibition [30,38]. The reaction products of both the synthetic dye and mediator might result in a decrease in laccase activity. In particular, the free radicals generated in the laccase-mediator system have been proven to have an adverse impact on laccase activity [45–47]. As the recyclability of Lac@Cu5/mZIF-8 is relatively low during batch-mode operation, it may be more suitable for use in fluidized-bed or packed-bed bioreactors under continuous mode [48].

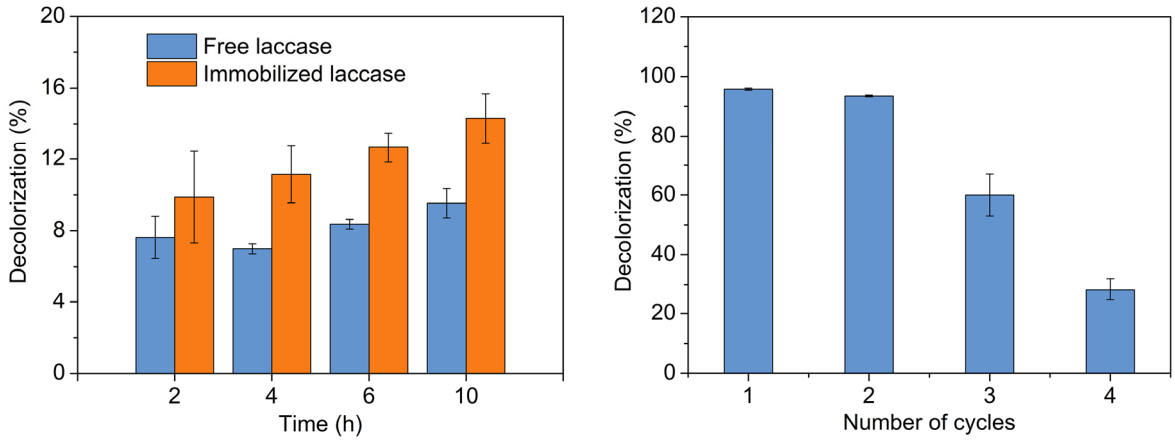


**Figure 5.** The decolorization of reactive black 5 by laccase. (**a**) The dye was decolorized by the free and immobilized laccase in the absence of a mediator; (**b**) the reusability of immobilized laccase in dye decolorization.

### *3.5. Identification of Decolorization Products*

To elucidate the decolorization mechanism of reactive black 5, the transformation products (TPs) were identified using LC-MS. Generally, reactive black 5 is degraded through the cleavage of the azo bond, resulting in the formation of 1,2,7-triamino-8-hydroxynaphthalene-3,6-disulfonic acid (Mw = 349.3) and 2-(4-aminobenzene-sulphonyl)-ethoxy-sulphonic acid (Mw = 281.3) [49–51]. Except for the cleavage of -N=N- bonds under reductive conditions, the most labile sites for the oxidative attack of reactive black 5 include the C1, C4, C9, C15, C21, and C24 sites. Therefore, the oxidation of reactive black 5 leads to the cleavage of C(4)-N(7), C(9)-N(8), C(15)-N(19), and C(21)-N(20) bonds. About four transformation products (TPs) of reactive black 5 were identified after treatment via the immobilized laccase–mediator system, and the possible degradation mechanism of reactive black 5 was proposed (Scheme 1). TP1 was formed via the cleavage of C(9)-N(8)

and C(15)-N(19) bonds, which has been detected in reactive black 5 degradation by laccase from *Weissella viridescens* [52] and laccase from *Cyathus bulleri* [53]. Meanwhile, the breakage of C-N bonds produced an intermediate, which was subsequently transformed into TP2 through hydroxylation. The product TP3 was generated via the cleavage of the azo bonds and the C(4)-N(7) or C(21)-N(20) bond. Then, it was decomposed to TP4 via deamination, hydroxylation, and desulfonation [52]. Based on the above results, the decolorization of reactive black 5 was achieved through non-specific oxidative attack, which was mediated by the free radical of acetosyringone generated via laccase catalysis. The main mechanism of reactive black 5 decolorization by Lac@Cu5/mZIF-8 included oxidative cleavage, hydroxylation, deamination, and desulfonation. The suggested mechanism was in agreement with previous reports on reactive black 5 decolorization [52–54].

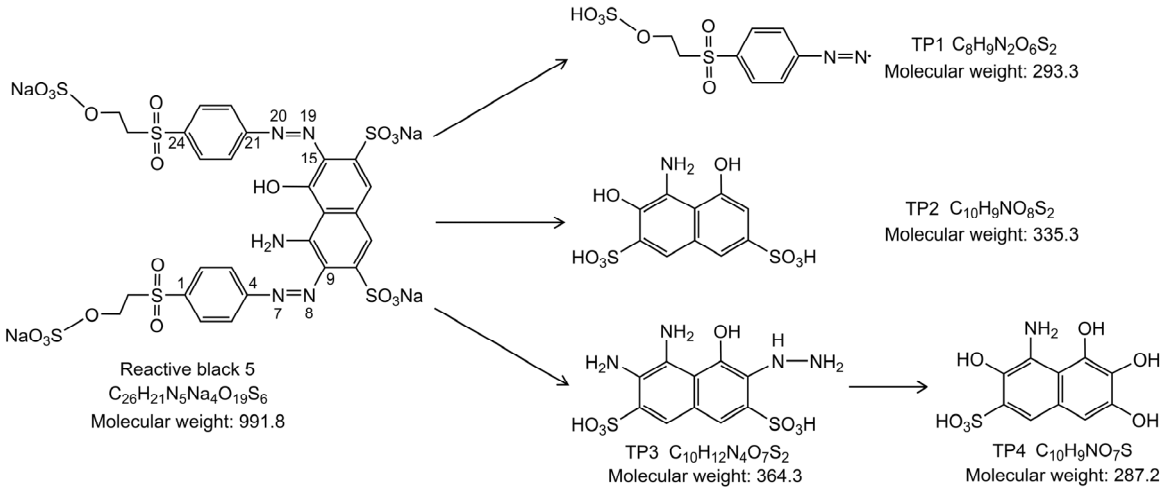


**Scheme 1.** The proposed decolorization mechanism of reactive black 5 via the immobilized laccase-mediator system.

## 4. Conclusions

In summary, we synthesized copper-doped modified ZIF-8 for laccase immobilization. The immobilization matrix (Cu5/mZIF-8) was obtained through lowering the precursor ratio of ZIF-8 as well as the incorporation of copper. Compared with ZIF-8, Cu5/mZIF-8 had a different morphology and size and provided an improved activity recovery for laccase encapsulation. The immobilized laccase displayed a higher catalytic activity in organic solvents than that of the free enzyme. Lac@Cu5/mZIF-8 could efficiently decolorize reactive black 5 in the presence of the mediator and could be recycled in dye decolorization. The transformation products of reactive black 5 were identified, and the major reaction pathways were proposed, with the possible mechanisms including oxidative cleavage, hydroxylation, deamination, and desulfonation.

**Author Contributions:** Conceptualization, S.Y.; methodology, S.Y. and Y.L.; validation, S.Y. and Y.L.; formal analysis, S.Y., Y.L., D.D. and X.J.; investigation, S.Y. and Y.L.; resources, S.Y., R.W. and H.L.; data curation, S.Y. and Y.L.; writing—original draft preparation, S.Y.; writing—review and editing, S.Y., D.D., R.W., X.J. and H.L.; visualization, S.Y.; supervision, S.Y. and H.L.; project administration, S.Y. and H.L.; funding acquisition, S.Y. All authors have read and agreed to the published version of the manuscript.

**Funding:** This research was funded by the Planned Science–Technology Project of Inner Mongolia Autonomous Region (grant number: 2022YFXZ0037) and the Major Science and Technology Project of Ordos City (grant number: 2022EEDSKJZDZX014).

**Data Availability Statement:** Not applicable.

**Conflicts of Interest:** The authors declare no conflict of interest.

## References


1. Solayman, H.M.; Hossen, M.A.; Aziz, A.A.; Yahya, N.Y.; Leong, K.H.; Sim, L.C.; Monir, M.U.; Zoh, K.D. Performance evaluation of dye wastewater treatment technologies: A review. *J. Environ. Chem. Eng.* **2023**, *11*, 109610. [CrossRef]
2. Alsukaibi, A.K.D. Various approaches for the detoxification of toxic dyes in wastewater. *Processes* **2022**, *10*, 1968. [CrossRef]
3. Rathi, B.S.; Kumar, P.S. Sustainable approach on the biodegradation of azo dyes: A short review. *Curr. Opin. Green Sustain. Chem.* **2022**, *33*, 100578. [CrossRef]
4. Selvaraj, V.; Karthika, T.S.; Mansiya, C.; Alagar, M. An over review on recently developed techniques, mechanism and intermediate involved in the advanced azo dyes degradation for industrial applications. *J. Mol. Struct.* **2021**, *1224*, 129195. [CrossRef]
5. Sarkar, S.; Banerjee, A.; Halder, U.; Biswas, R.; Bandopadhyay, R. Degradation of synthetic azo dyes of textile industry: A sustainable approach using microbial enzymes. *Water Conserv. Sci. Eng.* **2017**, *2*, 121–131. [CrossRef]
6. Wong, J.K.H.; Tan, H.K.; Lau, S.Y.; Yap, P.S.; Danquah, M.K. Potential and challenges of enzyme incorporated nanotechnology in dye wastewater treatment: A review. *J. Environ. Chem. Eng.* **2019**, *7*, 103261. [CrossRef]
7. Mishra, A.; Takkar, S.; Joshi, N.C.; Shukla, S.; Shukla, K.; Singh, A.; Manikonda, A.; Varma, A. An integrative approach to study bacterial enzymatic degradation of toxic dyes. *Front. Microbiol.* **2022**, *12*, 802544. [CrossRef]
8. Pinheiro, L.R.S.; Gradíssimo, D.G.; Xavier, L.P.; Santos, A.V. Degradation of azo dyes: Bacterial potential for bioremediation. *Sustainability* **2022**, *14*, 1510. [CrossRef]
9. Dong, C.D.; Tiwari, A.; Anisha, G.S.; Chen, C.W.; Singh, A.; Haldar, D.; Patel, A.K.; Singhania, R.R. Laccase: A potential biocatalyst for pollutant degradation. *Environ. Pollut.* **2023**, *319*, 120999. [CrossRef]
10. Deska, M.; Kończak, B. Immobilized fungal laccase as "green catalyst" for the decolourization process—State of the art. *Process Biochem.* **2019**, *84*, 112–123. [CrossRef]
11. Han, Z.; Fan, X.; Yu, S.; Li, X.; Wang, S.; Lu, L. Metal-organic frameworks (MOFs): A novel platform for laccase immobilization and application. *J. Environ. Chem. Eng.* **2022**, *10*, 108795. [CrossRef]
12. Liang, W.; Wied, P.; Carraro, F.; Sumby, C.J.; Nidetzky, B.; Tsung, C.K.; Falcaro, P.; Doonan, C.J. Metal-organic framework-based enzyme biocomposites. *Chem. Rev.* **2021**, *121*, 1077–1129. [CrossRef] [PubMed]
13. Ihsanullah, I. Applications of MOFs as adsorbents in water purification: Progress, challenges and outlook. *Curr. Opin. Environ. Sci. Health* **2022**, *26*, 100335. [CrossRef]
14. Uddin, M.J.; Ampiaw, R.E.; Lee, W. Adsorptive removal of dyes from wastewater using a metal-organic framework: A review. *Chemosphere* **2021**, *284*, 131314. [CrossRef] [PubMed]
15. Knedel, T.O.; Ricklefs, E.; Schlüsener, C.; Urlacher, V.B.; Janiak, C. Laccase encapsulation in ZIF-8 metal-organic framework shows stability enhancement and substrate selectivity. *ChemistryOpen* **2019**, *8*, 1337–1344. [CrossRef]
16. Wu, X.; Yue, H.; Zhang, Y.; Gao, X.; Li, X.; Wang, L.; Cao, Y.; Hou, M.; An, H.; Zhang, L.; et al. Packaging and delivering enzymes by amorphous metal-organic frameworks. *Nat. Commun.* **2019**, *10*, 5165. [CrossRef]
17. Hu, C.; Bai, Y.; Hou, M.; Wang, Y.; Wang, L.; Cao, X.; Chan, C.W.; Sun, H.; Li, W.; Ge, J.; et al. Defect-induced activity enhancement of enzyme-encapsulated metal-organic frameworks revealed in microfluidic gradient mixing synthesis. *Sci. Adv.* **2020**, *6*, eaax5785. [CrossRef] [PubMed]
18. Feng, Y.; Du, Y.; Kuang, G.; Zhong, L.; Hu, H.; Jia, S.; Cui, J. Hierarchical micro- and mesoporous ZIF-8 with core-shell superstructures using colloidal metal sulfates as soft templates for enzyme immobilization. *J. Colloid Interf. Sci.* **2022**, *610*, 709–718. [CrossRef]
19. Ogata, A.F.; Rakowski, A.M.; Carpenter, B.P.; Fishman, D.A.; Merham, J.G.; Hurst, P.J.; Patterson, J.P. Direct observation of amorphous precursor phases in the nucleation of protein-metal-organic frameworks. *J. Am. Chem. Soc.* **2020**, *142*, 1433–1442. [CrossRef]
20. Wang, J.; Lu, L.; Feng, F. Improving the indigo carmine decolorization ability of a *Bacillus amyloliquefaciens* laccase by site-directed mutagenesis. *Catalysts* **2017**, *7*, 275. [CrossRef]
21. Wu, X.; Ge, J.; Yang, C.; Hou, M.; Liu, Z. Facile synthesis of multiple enzyme-containing metal-organic frameworks in a biomolecule-friendly environment. *Chem. Commun.* **2015**, *51*, 13408–13411. [CrossRef] [PubMed]
22. Martins, L.O.; Soares, C.M.; Pereira, M.M.; Teixeira, M.; Costa, T.; Jones, G.H.; Henriques, A.O. Molecular and biochemical characterization of a highly stable bacterial laccase that occurs as a structural component of the *Bacillus subtilis* endospore coat. *J. Biol. Chem.* **2002**, *277*, 18849–18859. [CrossRef] [PubMed]
23. Tong, L.; Huang, S.; Shen, Y.; Liu, S.; Ma, X.; Zhu, F.; Chen, G.; Ouyang, G. Atomically unveiling the structure-activity relationship of biomacromolecule-metal-organic frameworks symbiotic crystal. *Nat. Commun.* **2022**, *13*, 951. [CrossRef]
24. Bassanini, I.; Ferrandi, E.E.; Riva, S.; Monti, D. Biocatalysis with laccases: An updated overview. *Catalysts* **2021**, *11*, 26. [CrossRef]
25. Zhang, C.; You, S.; Zhang, J.; Qi, W.; Su, R.; He, Z. An effective in-situ method for laccase immobilization: Excellent activity, effective antibiotic removal rate and low potential ecological risk for degradation products. *Bioresour. Technol.* **2020**, *308*, 123271. [CrossRef] [PubMed]
26. Zhou, Y.; Yang, T.; Namivandi-Zangeneh, R.; Boyer, C.; Liang, K.; Chandrawati, R. Copper-doped metal-organic frameworks for the controlled generation of nitric oxide from endogenous S-nitrosothiols. *J. Mater. Chem. B* **2021**, *9*, 1059–1068. [CrossRef]
27. Sun, Y.; Zhao, Y.; Zhan, X.; Gao, R.; Chen, L.; Yu, J.; Wang, H.; Shi, H. A ZIF-8-derived copper-nitrogen co-hybrid carbon catalyst for peroxymonosulfate activation to degrade BPA. *Chemosphere* **2022**, *308*, 136489. [CrossRef]

28. Kinoshita, M.; Yanagida, S.; Gessei, T.; Monkawa, A. Precusor concentration effects on crystallite size and enzyme immobilization efficiency of Enzyme@ZIF-8 composite. *J. Cryst. Growth* **2022**, *600*, 126877. [CrossRef]
29. Qi, X.; Chen, Q.; Chang, Z.; Deng, Y. Breaking pore size limit of metal-organic frameworks: Bio-etched ZIF-8 for lactase immobilization and delivery in vivo. *Nano Res.* **2022**, *15*, 5646–5652. [CrossRef]
30. Pitzalis, F.; Carucci, C.; Naseri, M.; Fotouhi, L.; Magner, E.; Salis, A. Lipase encapsulation onto ZIF-8: A comparison between biocatalysts obtained at low and high zinc/2-methylimidazole molar ratio in aqueous medium. *ChemCatChem* **2018**, *10*, 1578–1585. [CrossRef]
31. Kida, K.; Okita, M.; Fujita, K.; Tanaka, S.; Miyake, Y. Formation of high crystalline ZIF-8 in an aqueous solution. *CrystEngComm* **2013**, *15*, 1794–1801. [CrossRef]
32. Ökte, A.N.; Tuncel, D. Improved adsorption capacity and photoactivity of ZnO-ZIF-8 nanocomposites. *Catal. Today* **2021**, *361*, 191–197.
33. Zhang, Y.; Xie, Z.; Wang, Z.; Feng, X.; Wang, Y.; Wu, A. Unveiling the adsorption mechanism of zeolitic imidazolate framework-8 with high efficiency for removal of copper ions from aqueous solutions. *Dalton Trans.* **2016**, *45*, 12653–12660. [CrossRef] [PubMed]
34. Júnior, O.B.; Bedran-Russo, A.; Flor, J.B.S.; Borges, A.F.S.; Ximenes, V.F.; Frem, R.C.G.; Lisboa-Filho, P.N. Encapsulation of collagenase within biomimetically mineralized metal-organic frameworks: Designing biocomposites to prevent collagen degradation. *New J. Chem.* **2019**, *43*, 1017–1024. [CrossRef]
35. Chen, G.; Kou, X.; Huang, S.; Tong, L.; Shen, Y.; Zhu, W.; Zhu, F.; Ouyang, G. Modulating the biofunctionality of metal-organic-framework-encapsulated enzymes through controllable embedding patterns. *Angew. Chem. Int. Edit.* **2020**, *59*, 2867–2874. [CrossRef]
36. Liang, Z.; Yang, Z.; Yuan, H.; Wang, C.; Qi, J.; Liu, K.; Cao, R.; Zheng, H. A protein@metal-organic framework nanocomposite for pH-triggered anticancer drug delivery. *Dalton Trans.* **2018**, *47*, 10223–10228. [CrossRef] [PubMed]
37. Han, Z.; Wang, H.; Zheng, J.; Wang, S.; Yu, S.; Lu, L. Ultrafast synthesis of laccase-copper phosphate hybrid nanoflowers for efficient degradation of tetracycline antibiotics. *Environ. Res.* **2023**, *216*, 114690. [CrossRef] [PubMed]
38. Patil, P.D.; Yadav, G.D. Rapid in situ encapsulation of laccase into metal-organic framework support (ZIF-8) under biocompatible conditions. *ChemistrySelect* **2018**, *3*, 4669–4675. [CrossRef]
39. Dlamini, M.L.; Lesaoana, M.; Kotze, I.; Richards, H.L. Zeolitic imidazolate frameworks as effective crystalline supports for *aspergillus*-based laccase immobilization for the biocatalytic degradation of carbamazepine. *Chemosphere* **2023**, *311*, 137142. [CrossRef]
40. Farajzadeh-Dehkordi, N.; Zahraei, Z.; Farhadian, S.; Gholamian-Dehkordi, N. The interactions between reactive black 5 and human serum albumin: Combined spectroscopic and molecular dynamics simulation approaches. *Environ. Sci. Pollut. Res.* **2022**, *29*, 70114–70124. [CrossRef]
41. Zeng, X.; Cai, Y.; Liao, X.; Zeng, X.; Luo, S.; Zhang, D. Anthraquinone dye assisted the decolorization of azo dyes by a novel *Trametes trogii* laccase. *Process Biochem.* **2012**, *47*, 160–163. [CrossRef]
42. Schubert, M.; Muffler, A.; Mourad, S. The use of a radical basis neural network and genetic algorithm for improving the efficiency of laccase-mediated dye decoulourization. *J. Biotechnol.* **2012**, *161*, 429–436. [CrossRef] [PubMed]
43. Yang, J.; Xu, H.; Zhao, J.; Zhang, N.; Xie, J.; Jiang, J. Isolation of *Bacillus* sp. with high laccase activity for green biodecolorization of synthetic textile dyes. *Water Sci. Technol.* **2022**, *86*, 777–786. [CrossRef]
44. Wu, X.; Yang, C.; Ge, J.; Liu, Z. Polydopamine tethered enzyme/metal-organic framework composites with high stability and reusability. *Nanoscale* **2015**, *7*, 18883–18886. [CrossRef] [PubMed]
45. Kurniawati, S.; Nicell, J.A. Efficacy of mediators for enhancing the laccase-catalyzed oxidation of aqueous phenol. *Enzyme Microb. Technol.* **2007**, *41*, 353–361. [CrossRef]
46. Fillat, A.; Colom, J.F.; Vidal, T. A new approach to the biobleaching of flax pulp with laccase using natural mediators. *Bioresour. Technol.* **2010**, *101*, 4104–4110. [CrossRef]
47. Rehmann, L.; Ivanova, E.; Gunaratne, H.Q.N.; Seddon, K.R.; Stephens, G. Enhanced laccase stability through mediator partitioning into hydrophobic ionic liquids. *Green Chem.* **2014**, *16*, 1462. [CrossRef]
48. Zhang, X.J.; Qi, F.Y.; Qi, J.M.; Yang, F.; Shen, J.W.; Cai, X.; Liu, Z.Q.; Zheng, Y.G. Efficient enzymatic synthesis of *L*-ascorbyl palmitate using *Candida antarctica* lipase B-embedded metal-organic framework. *Biotechnol. Progress* **2022**, *38*, e3218. [CrossRef]
49. Zheng, X.; Xie, X.; Liu, Y.; Cong, J.; Fan, J.; Fang, Y.; Liu, N.; He, Z.; Liu, J. Deciphering the mechanism of carbon sources inhibiting recolorization in the removal of refractory dye: Based on an untargeted LC-MS metabolomics approach. *Bioresour. Technol.* **2020**, *307*, 123248. [CrossRef]
50. Al-Tohamy, R.; Kenawy, E.R.; Sun, J.; Ali, S.S. Performance of a newly isolated salt-tolerant yeast strain *Sterigmatomyces halophilus* SSA-1575 for azo dye decolorization and detoxification. *Front. Microbiol.* **2020**, *11*, 1163. [CrossRef]
51. Joksimović, K.; Kodranov, I.; Randjelović, D.; Beškoski, L.S.; Radulović, J.; Ljević, M.; Manojlović, D.; Beškoski, V.P. Microbial fuel cells as an electrical energy source for degradation followed by decolorization of Reactive Black 5 azo dye. *Bioelectrochemistry* **2022**, *145*, 108088. [CrossRef] [PubMed]
52. Nadaroglu, H.; Mosber, G.; Gungor, A.A.; Adıguzel, A.; Adiguzel, A. Biodegradation of some azo dyes from wastewater with laccase from *Weissella viridescens* LB37 immobilized on magnetic chitosan nanoparticles. *J. Water Process Eng.* **2019**, *31*, 100866. [CrossRef]

53. Vats, A.; Mishra, S. Identification and evaluation of bioremediation potential of laccase isoforms produced by *Cyathus bulleri* on wheat bran. *J. Hazard. Mater.* **2018**, *344*, 466–479. [CrossRef]
54. Zheng, Q.; Dai, Y.; Han, X. Decolorization of azo dye C.I. Reactive Black 5 by ozonation in aqueous solution: Influencing factors, degradation products, reaction pathway and toxicity assessment. *Water Sci. Technol.* **2016**, *73*, 1500–1510. [CrossRef] [PubMed]